LABORATOIRE

INFORMATIQUE, SIGNAUX ET SYSTÈMES
DE SOPHIA ANTIPOLIS
UMR 6070

NONINVASIVE ASSESSMENT OF THE COMPLEXITY AND STATIONARITY OF THE ATRIAL WAVEFRONT PATTERNS DURING ATRIAL FIBRILLATION

Pietro Bonizzi, Olivier Meste, Vicente Zarzoso, Francisco Castells

Equipe SIGNAL

Rapport de recherche
ISRN I3S/RR–2009-15–FR

Octobre 2009

Laboratoire d'Informatique de Signaux et Systèmes de Sophia Antipolis - UNSA-CNRS
2000, rte.des Lucioles – Les Algorithmes – Bât Euclide B – B.P. 121 – 06903 Sophia-Antipolis Cedex – France
Tél.: 33 (0)4 92 94 27 01 – Fax: 33 (0)4 92 94 28 98 – www.i3s.unice.fr
UMR6070

RÉSUMÉ :

MOTS CLÉS :

Fibrillation auriculaire, Mappage des potentiels de surface du corps, Analyse des composants principaux, Topographies spatiales

ABSTRACT:

The degree of organization in the atrial activity (AA) during atrial fibrillation (AF) has been observed to be related to its chronification and then potentially to better lead its treatment. Motivated by this potential relevance in clinical making decision, a number of previous studies have attempted to distinguish between organized and disorganized states of AF by analyzing atrial electrograms. More recent works have attempted a noninvasive evaluation of AF organization through ECG recordings, demonstrating the possibility of visually evaluating different activation patterns in AF patients, similar to those observed invasively, but exploiting body surface potential maps (BSPM) recordings. This work puts forward a novel automated approach to noninvasively evaluate the degree of spatio-temporal organization in the AA during AF. A quantitative evaluation of AA organization is carried out by means of PCA by assessing the reflection of the spatial complexity and temporal stationarity of the wavefront patterns propagating inside the atria on the surface ECG. Complexity and stationarity are investigated through newly-proposed parameters evaluating the structure of the mixing matrices derived by the PCA of the different AA segments across the BSPM recording. The discriminative power of the parameters in distinguishing among different types of AF is also analyzed. The results suggest that automated analysis and classification of AF organization in surface recordings is indeed possible and strongly support the appropriateness of signal processing approaches exploiting spatial diversity in AF analysis.

KEY WORDS :

Atrial fibrillation, Body surface potential mapping, Principal component analysis, Spatial topographies

Noninvasive Assessment of the Complexity and Stationarity of the Atrial Wavefront Patterns During Atrial Fibrillation

Pietro Bonizzi*, Olivier Meste, Vicente Zarzoso, Francisco Castells

Abstract

The degree of organization in the atrial activity (AA) during atrial fibrillation (AF) has been observed to be related to its chronification and then potentially to better lead its treatment. Motivated by this potential relevance in clinical making decision, a number of previous studies have attempted to distinguish between organized and disorganized states of AF by analysing atrial electrograms. More recent works have attempted a noninvasive evaluation of AF organization through ECG recordings, demonstrating the possibility of visually evaluating different activation patterns in AF patients, similar to those observed invasively, but exploiting body surface potential maps (BSPM) recordings. This work puts forward a novel automated approach to noninvasively evaluate the degree of spatio-temporal organization in the AA during AF. A quantitative evaluation of AA organization is carried out by means of PCA by assessing the reflection of the spatial complexity and temporal stationarity of the wavefront patterns propagating inside the atria on the surface ECG. Complexity and stationarity are investigated through newly-proposed parameters evaluating the structure of the mixing matrices derived by the PCA of the different AA segments across the BSPM recording. The discriminative power of the parameters in distinguishing among different types of AF is also analysed. The results suggest that automated analysis and classification of AF organization in surface recordings is indeed possible and strongly support the appropriateness of signal processing approaches exploiting spatial diversity in AF analysis.

Index Terms

Atrial fibrillation (AF), BSPM, PCA, spatial topographies.

I. Introduction

DURING atrial fibrillation (AF) the atrial tissue is activated by multiple wavelets showing uncoordinated patterns, appearing as an irregular heart rhythm disturbance with no detectable relationship between consecutive beats. Because of that, AF has often been studied as a random phenomenon [1], [2]. Nonetheless, several studies have demonstrated the presence of organization of atrial activation processes during AF, indicating that a certain degree of local organization exists during AF, likely caused by deterministic mechanisms of activation [3], and inversely depending on the chronification of the pathology [4]. Moreover, several authors have observed that different types of AF patterns could be concurrently present at different locations during experimental AF [5], [6]. Hence, from a pathophysiological point of view it can be inferred that AF is not a homogeneous arrhythmia [7]. Different strategies for its treatment are selected in respect to the duration of its episodes [8], and their efficacy can also be influenced by the degree of organization in the atrial activity (AA) [9].

Motivated by their potential relevance in clinical making decision, a number of previous studies have attempted to distinguish between organized and disorganized states of AF by analysing atrial electrograms [10], [11]. Konings *et al.*, in the attempt of reconstructing and classifying the patterns of human right atrial activations during electrically induced AF, defined three types of AF based on the degree of complexity of atrial activations. An increasing fractionation of the observed atrial activations was associated with an increasing number of interacting wavefronts and then a higher complexity. Faes *et al.* ([12]) used principal component analysis (PCA) in order to quantify the number of dominant components in the atrial activations, as an estimate of the AA complexity. These authors noticed that single-lead electrograms recorded at different sites and presenting different AA organization were shown to be represented by a different number of principal components, with a reduced number of components representing more organized AA [12].

On the other side, since surface electrocardiogram (ECG) has been demonstrated to be a valuable tool for studying AF [13], more recent works [14] have attempted a noninvasive evaluation of AF organization through ECG recordings, demonstrating the possibility of visually evaluating different activation patterns in AF patients, similar to those observed invasively by Konings *et al.* [11], but exploiting body surface potential maps (BSPM) recordings [15]. BSPM is a technique previously applied to the study of many cardiac diseases [16], [17], and having the advantage over the conventional ECG of a much higher spatial resolution. By means of it, Guillem *et al.* observed interindividual differences of surface atrial fibrillatory activation patterns characterized by an excellent short-term reproducibility [14].

In line with this study, this work puts forward a new automated method for noninvasively evaluating the degree of spatio-temporal organization of the atrial activations during AF. By means of PCA, AA organization is evaluated quantitatively by

*P. Bonizzi, V. Zarzoso and O. Meste are with the Laboratoire I3S, UNSA/CNRS, Sophia Antipolis, 06903 France e-mail: bonizzi@i3s.unice.fr.
F. Castells is with ITACA - Bioingenieria, Universitat Politecnica de Valencia, 46022 España.

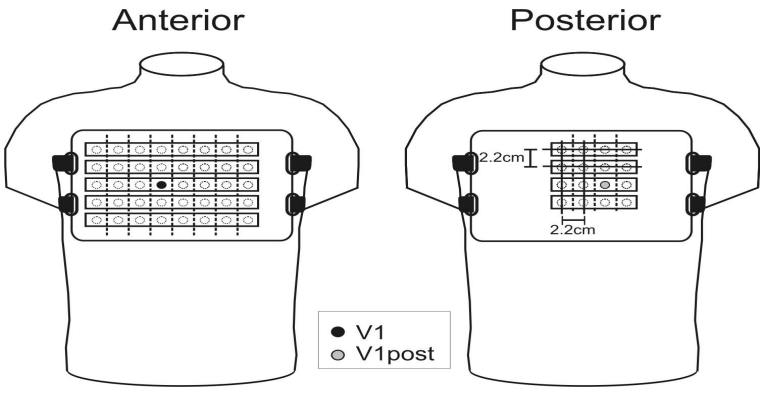

(a)

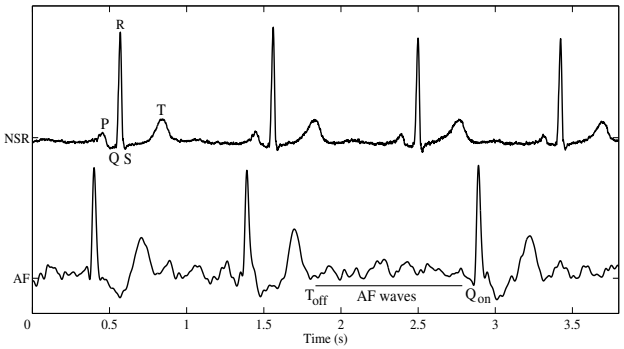

(b)

Fig. 1. (a) Arrangement of the electrodes and belt used for their attachment to the patient. Electrode positions are represented as open circles while V1 and V1post are denoted by black and grey circles, respectively. Electrodes were placed around V1 and V1post as a uniform grid. (b) Definition of the different cardiac waves and intervals of interest. At the top, example of normal sinus rhythm ECG recording (NSR), showing the different cardiac waves. At the bottom, example of ECG recording during AF, showing a TQ interval (off:offset; on:onset).

assessing the spatial complexity and temporal stationarity of atrial activation patterns from the analysis of BSPM recordings. PCA has been attested to be a valuable tool both for addressing diverse issues in ECG analysis [18], and for quantifying AA organization complexity in invasive recordings [12]. Moreover, the spatial information derivable from the PCA of the different ECG components in a multi-lead recordings has turned out to be useful as a first step in the extraction of the AA from surface ECG [19], [20]. Hence, complexity and stationarity are quantified with novel parameters that assess the structure of the mixing matrices derived by the PCA of the different AA segments in the BSPM recording. Furthermore, the ability of these parameters to distinguish among different degrees of AF organization is explored, in order to achieve a noninvasive classification of the AF. Results are then compared to those reported by Guillem *et al.* on the same dataset [14], who performed a visual classification of AF making use of a noninvasive method based on wavefront propagation mapping, according to the same criteria and terminology for classification as those of Konings *et al.* [11], although applied to surface recordings instead of electrograms. The paper is outlined as follows: the method is presented in Section II, the results in Section III, and a discussion of the method in terms of ability in describing the degree of AF organization and in performing AF classification is found in Section IV.

II. Materials and Methods

A. BSPM Data and Acquisition System

The same dataset composed of 14 patients as the one introduced in [14] was employed in this study. One BSPM signal was recorded for each patient. All recordings presented persistent AF. The acquisition system employed in [14] consisted of a total of 56 chest and back leads acquired simultaneously for each subject. Chest leads (n=40) were arranged as a grid around V1 with an interelectrode distance of 2.2 cm, while back leads (n=16) were arranged in a similar way around a lead opposite to V1 (V1post), as shown in Fig. 1(a). Only the first 60s of each BSPM recording were analysed in this study.

Signals were acquired at a sampling frequency of 2,048 Hz, with a resolution of 1 μV and an anti-aliasing low-pass bandwidth of DC-500 Hz.

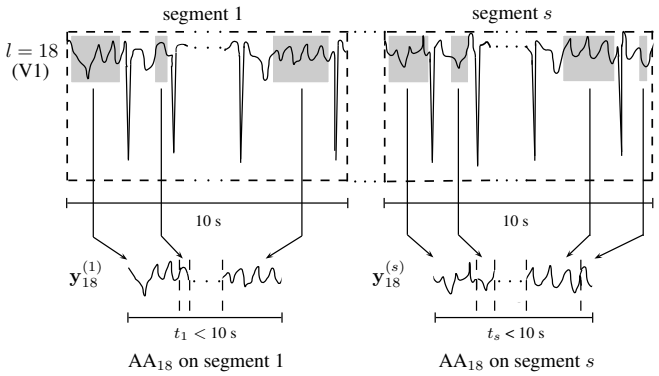

Fig. 2. Schematic example of AA recording generation on lead 18 only (lead V1). Each lead recording is split in consecutive and non-overlapping 10s segments, and all TQ intervals inside a specific segment s are joint in order to get the AA recording $\mathbf{Y}^{(s)}$.

B. ECG Signal Preprocessing

Signals were processed by applying a third-order zerophase high-pass Chebyshev filter with a -3 dB cut off frequency at 0.5 Hz to remove baseline wandering due to physiologically irrelevant low frequency signal interference (< 1 Hz), like breathing influence [21], followed by a third-order zerophase low-pass Chebyshev filter with a -3 dB cut off frequency at 100 Hz to remove high frequency noise, like myoelectric artifacts. Finally, a zerophase notch filter at 50 Hz was used to suppress power line interference.

All leads in all recordings were visually inspected. Leads presenting noticeable noise contributions, typically due to a transient loss of contact in one electrode, were discarded. This preserved the following PCA from being impaired by the abnormal statistical behaviour of these observations. Since the average of discarded leads was 1 per recording, and taking into account the large number of leads at our disposal, we considered the number of remaining leads sufficient for subsequent analysis, avoiding the interpolation of the discarded leads.

C. Atrial Activity Recordings

In this study only the TQ segments in the BSPM recording were analysed. For this purpose, the R wave peak, the Q wave onset, and the T wave offset were detected (see Fig. 1(b) for the definition of the different cardiac waves). Each BSPM lead recording was split in 6 consecutive 10s-length intervals, and an AA signal was obtained for each interval concatenating only the TQ segments inside it. In this way, for each $56-$lead BSPM recording we constructed 6 consecutive $56-$lead AA recordings.

Each lead l in the sth AA recording (with $s = 1, \ldots, 6$) is represented by a row vector:

$$\mathbf{y}_l^{(s)} = [y_l^{(s)}(1), \ldots, y_l^{(s)}(N)] \tag{1}$$

where N is the number of samples inside the interval. Then, the entire ensemble of leads is compactly represented by the $n \times N$ matrix:

$$\mathbf{Y}^{(s)} = \begin{bmatrix} \mathbf{y}_1^{(s)} \\ \vdots \\ \mathbf{y}_{56}^{(s)} \end{bmatrix}$$

A schematic example of this procedure is illustrated in Fig. 2 for the sake of clarity, for lead $l = 18$ only, corresponding to V1.

D. Principal Component Analysis

ECG is a signal with a high spatial redundancy [18]. One manner to analyse the complex information contained in the ECG is to transform the original set of signals in a set of components by minimizing the redundancy among them. This can be achieved by PCA. Indeed, spatial uncorrelation provided by PCA involves a linear transformation of the mean corrected observed signals $\mathbf{Y} \in \mathbb{R}^n$, which produces a set of mutually uncorrelated waveforms with unit variance $\mathbf{X} \in \mathbb{R}^m$ with ($m \leq n$). The PCA of $\mathbf{Y}$ yields an estimate of the following noiseless model:

$$\mathbf{Y} = \mathbf{M}\mathbf{X} \Rightarrow \mathbf{X} = \left[\mathbf{M}^{\mathrm{T}}\mathbf{M}\right]^{-1}\mathbf{M}^{\mathrm{T}}\mathbf{Y} = \mathbf{M}^{\sharp}\mathbf{Y} \tag{2}$$

where $\mathbf{X}$ is an estimate of the true vector of the unknown components, $\mathbf{M}$ is the mixing matrix, and symbol $^{\sharp}$ stands for the pseudo-inverse operator. Even if the model in (2) is supposed to be noiseless, this model is usually employed in the presence

of noise as well. In that case, the number of principal components (PCs) generally matches the number of measured signals, and the last PCs are associated with noise. The *i*th column of $\mathbf{M}$ represents the source direction or spatial topography that links the *i*th component of $\mathbf{X}$ with the observed signals $\mathbf{Y}$. The spatial topography describes the relative contribution of the uncorrelated components at each electrode. PCA reduces the dataset of the observed signals to few representative components. The mixing matrix $\mathbf{M}$ can be obtained, e.g., from the singular value decomposition of the observation matrix $\mathbf{Y} = \mathbf{U}\mathbf{\Sigma}\mathbf{V}^{\mathbf{T}}$, where $\mathbf{M} = \mathbf{U}\mathbf{\Sigma}\sqrt{N}$. In addition, each PC is associated with a singular value σ_i, which indicates how representative is the *i*th PC in the global data ensemble. The PCs are usually arranged so that the singular value sequence appears in a decreasing order. This sequence reflects some information regarding interlead variability. In fact, a fast fall-down is associated to a low spatial variability, while a slow fall-down indicates a large spatial variability. The ability of PCA to concentrate the original information in only k components (number of significant components, ($k < m$)) can be assessed by the cumulative normalized variance v_k, an index that reflects how well the subset of the first k principal components approximates the ensemble of original observations in energy terms:

$$v_k \;=\; \frac{\sum_{i=1}^{k} \sigma_i^2}{\sum_{i=1}^{m} \sigma_i^2} \tag{3}$$

E. Assessment of Spatio-Temporal Organization of the AA

The degree of spatio-temporal organization of the AA during AF is noninvasively evaluated as the spatial complexity and temporal stationarity of the wavefront pattern propagating inside the atria, supposed to be reflected on the surface ECG. These two aspects are investigated through the structure of the mixing matrices derived by the PCA of the different AA segments in the BSPM recording, introduced in Section II-C. Complexity will be analysed in terms of the number of components required for explaining 95% of the variance of the underlying AA, while stationarity in terms of the repetitiveness of the mixing matrix along the BSPM recording, as subsequently described in Sections II-E1 and II-E2, respectively.

1) AA Spatial Complexity: A more organized AA is supposed to be reflected in the structure of the PCA mixing matrix in terms of a lower number of significant components needed to describe its variance. To this end, the average number of significant components k required to explain 95% of the variance ($k_{0.95}$) is considered a first indication of the AF organization. Then, for a given patient, the PCA of the *s*th segment yields an estimate of the noiseless BSS model 2:

$$\mathbf{Y}^{(s)} \;=\; \mathbf{M}^{(s)}\mathbf{X}^{(s)} \tag{4}$$

and the average number $k_{0.95}$ is derived over all PCA mixing matrices $\mathbf{M}^{(s)}$. The underlying idea is that when the eigenvalues associated to the first components are much larger than those associated to other components, the ensemble exhibits a low morphological variability, whereas a slow fall-down of the principal components values indicates a large variability, and so a higher complexity of the underlying AA.

2) AA Temporal Stationarity: To increase the discriminative power of the analysis, the data in the *s*th segment are reprojected on the spatial topographies associated with the $k_{0.95}$ most significant principal components of the initial segment, stored in the first k columns of matrix $\mathbf{M}^{(1)}$. The projection can then be expressed as:

$$\begin{aligned} \hat{\mathbf{Y}}^{(s)} &= \mathbf{M}_k^{(1)} \left[(\mathbf{M}_k^{(1)})^{\mathrm{T}} \mathbf{M}_k^{(1)} \right]^{-1} (\mathbf{M}_k^{(1)})^{\mathrm{T}} \mathbf{Y}^{(s)} \\ &= \mathbf{M}_k^{(1)} (\mathbf{M}_k^{(1)})^{\sharp} \mathbf{Y}^{(s)} \end{aligned} \tag{5}$$

where T stands for the transpose operator. From this relationship, the normalized error between the data present in the *s*th segment and their reconstruction from the $k_0.95$ most significant topographies of the initial segment is computed. This error measures the temporal stationarity or repetitiveness of the AA observed in the BSPM recording, as the ability of $\mathbf{M}^{(1)}$ derived for the initial segment $\mathbf{Y}^{(1)}$ to retrieve the AA components of subsequent segments. It is assumed as inversely dependent on the AF organization, and then directly on its complexity. This model looks similar to the one proposed by Rieta *et al.* in [22], used to corroborate that an AF recording satisfies the independent component analysis model (in terms of stationarity of the projection coefficients). Differently from this model, mixing matrix repetitiveness is herein analysed in terms of similarities between the original observations and the reconstructed ones. Indeed, the closer matrices $\mathbf{M}^{(s)}$ and $\mathbf{M}^{(1)}$ are, the closer the reconstructed observations with the originals are. Hence, more organized states of AF are reflected on an increased repetitiveness of the principal spatial topographies across the surface recording. An example of the procedure is illustrated in Fig. 3.

The reconstruction error is computed in terms of normalized mean squared error ($NMSE_{k_{0.95}}$) on lead 18, corresponding to V_1 (this is the lead from the standard 12-lead ECG that usually exhibits atrial fibrillatory waves with larger amplitude). Subscript index 18 is substituted by V1 in the following for clarity:

$$\mathrm{NMSE}_{k_{0.95}}^{(s)} \;=\; \frac{\sum_{i=1}^{N} (y_{V1}^{(s)}(i) - \hat{y}_{V1}^{(s)}(i)^2)}{\sum_{i=1}^{N} (y_{V1}^{(s)}(i)^2)} \tag{6}$$

where $\mathbf{y}_{V1}^{(s)}$ denotes the reference signal, $\hat{\mathbf{y}}_{V1}^{(s)}$ an estimate of it, and N its length. High values indicate notable differences between the original and reconstructed AA signals, while values close to zero are associated with very similar AA signals.

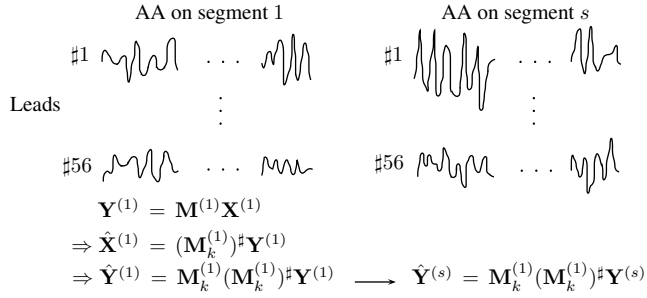

Fig. 3. Example of the proposed procedure. AA recording on segment s ($\mathbf{Y}^{(s)}$) is projected on the spatial topographies associated with the most significant principal component of the initial segment $\mathbf{M}_k^{(1)}$, giving the projection $\hat{\mathbf{Y}}^{(s)}$.

Additionally to the experiment previously describe, a further study is carried out considering a fixed number of topographies for all patients, instead of $k_{0.95}$. More specifically, in this study we consider $k = 3$, since the three most significant components are supposed to contain most of the information of the ECG, at least in signals with low complexity. Indeed, some studies claim that the ECG can be well explained using only three components, so that just with the first three eigenvectors and eigenvalues the essential information of the ECG is contained. This property motivated, e.g., the definition of the T-wave residuum [23], which accounts for the proportion of the data that lies out of the aforementioned three dimensional space where cardiac signals have been usually represented, such as the vectorcardiogram (VCG). The idea behind the study proposed here is that patients with more organized AA patterns will probably require a lower number of components to represent 95% of the variance in the original data. Similarly, if a fixed number of components is selected, a better reconstruction is expected in the same patient group. As a result, the reconstruction error is once more computed and defined as $\text{NMSE}_{k=3}$. With this experiment, the effects of the spatial complexity and temporal reproducibility of AA patterns are joined in a single parameter, and therefore, it is expected to emphasize the differences between more organized and less organized AF groups.

In order to enhance the hypothesis that complexity held in the analysed signals is really something related to AA, two additional analysis are carried out. Firstly, the influence of the noise on the complexity of the signal is investigated looking at the correlations of both $k_{0.95}$ and $\text{NMSE}_{k=3}$, respectively, with the energy of the AA segments. Second, the correlation between the difference $\text{NMSE}_{k_{0.95}} - \text{NMSE}_{k=3}$ and $k_{0.95}$ is investigated in order to test the influence of the method on the increase of the correlation between complexity and NMSE when fixing $k = 3$.

F. Noninvasive Classification of AF

The spatio-temporal analysis presented in Section II-E, can be seen as a new way for noninvasively assessing the degree of spatio-temporal organization of the AA during AF. Consequently, it appears worthy to explore the ability of parameters $k_{0.95}$ and NMSE to distinguish among different degrees of AF organization, in order to achieve a noninvasive classification of AF. To this extent, a cluster analysis is performed on the whole dataset in order to analyse the discriminatory power of $k_{0.95}$ and $\text{NMSE}_{k=3}$. A k-means algorithm for clustering is used, based on an iterative partitioning which minimized the sum, over all clusters, of the within-cluster sums of point-to-cluster-centroid distances. The standard metric chosen is the squared euclidean distance

$$d = \sum_{j=1}^{K}\sum_{i=1}^{N} \|g_i^{(j)} - c_j\|^2 \tag{7}$$

where $g_i^{(j)}$ is a data point of cluster j, c_j is the cluster center, and d is an indicator of the distance of the N data points from their respective cluster centers.

Results of the cluster analysis will be compared to those reported by Guillem *et al.* on the same dataset [14]. These authors performed a visual classification of AF making use of a noninvasive method based on wavefront propagation mapping, according to the same criteria and terminology for classification as those of Konings *et al.* [11], although applied to surface recordings instead of electrograms. Hence, according to [14], 6 patients have been classified as AF type I (single wavefront propagating across the body surface) and 8 as AF type II/III (no observable clear wavefront or multiple wavefronts that do not propagate across the body surface observed simultaneously). Results of the classification on each patient are summarized in Table I.

G. Statistical Analysis

Mean values of parameters $\text{NMSE}_{k_{0.95}}$ and $\text{NMSE}_{k=3}$ have been calculated for each patient averaging their values over segments $s = 2, \ldots, 6$. Mean values of parameter $k_{0.95}$ have been calculated for each patient averaging its values over segments $s = 1, \ldots, 6$. Pearson's coefficient r is calculated for each relation analysed in the study. Statistical significances have been evaluated by means of Whelchs t-test.

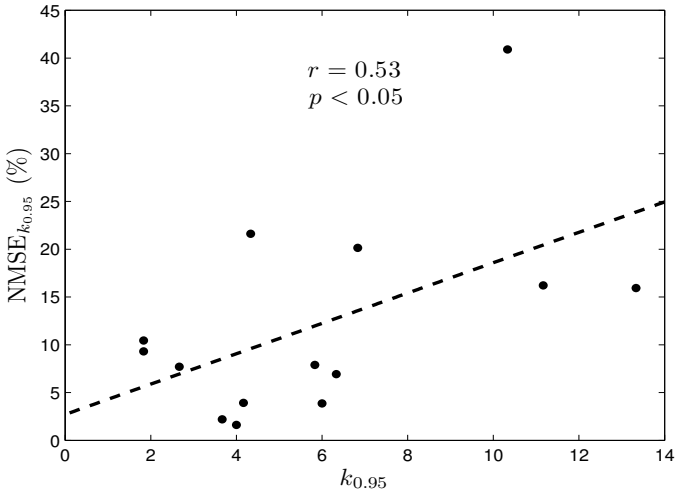

Fig. 4. Mean values of the parameters $k_{0.95}$ and $\mathrm{NMSE}_{k_{0.95}}$ for each patient, calculated as in Section II-G. Dashed line summarizes the linear interpolation. Values of the correlation coefficient r and its significance p are also reported.

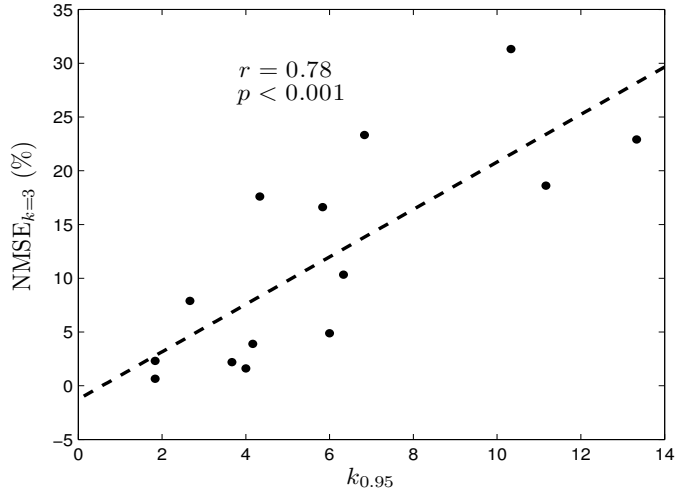

Fig. 5. Mean values of the parameters $k_{0.95}$ and $\mathrm{NMSE}_{k=3}$ for each patient, calculated as in Section II-G. Dashed line summarizes the linear interpolation. Values of the correlation coefficient r and its significance p are also reported.

III. RESULTS

A. Spatio-Temporal Organization of the AA during AF

To quantify the degree of spatio-temporal organization of the AA during AF, the structure of the mixing matrix derived by the PCA of the AA segments in the BSPM recording was analysed in terms of its complexity ($k_{0.95}$) and repetitiveness ($\mathrm{NMSE}_{k_{0.95}}$). Fig. 4 shows the averages of the two parameters calculated for each patient.

Correlation coefficient $r = 0.53 (> 0.5)$ underlines a positive correlation between $\mathrm{NMSE}_{k_{0.95}}$ and $k_{0.95}$, which is representative of the ensemble of the data ($p < 0.05$). This positive correlation points out the inverse correlation between stationarity and complexity, introduced in Section II-E. Selecting $k = 3$ most significant topographies of the initial segment, as introduced in Section II-E2, the average reconstruction errors ($\mathrm{NMSE}_{k=3}$) across the remaining segments between the data in the original segments and their projections on the 3 dominant principal topographies of the initial segment increased particularly in patients presenting higher complexity $k_{0.95}$ (> 4), as shown in Fig. 5. The significant increase ($p < 0.001$) in the correlation of the two parameters is underlined by the reciprocal increase in the correlation coefficient $r = 0.78$. AA signal reconstruction is generally better for signals showing low complexity. For each patient, mean NMSE was calculated averaging over segments

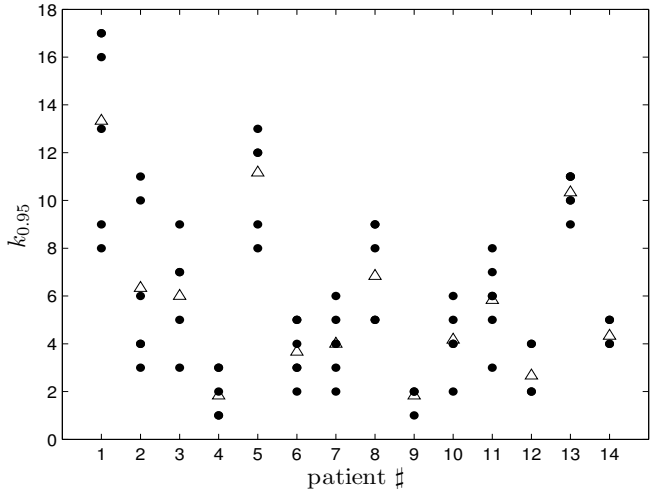

Fig. 6. Values of $k_{0.95}$ in segments 1 up to 6 for all patients in the dataset (•). Mean values are also shown for each patient (△).

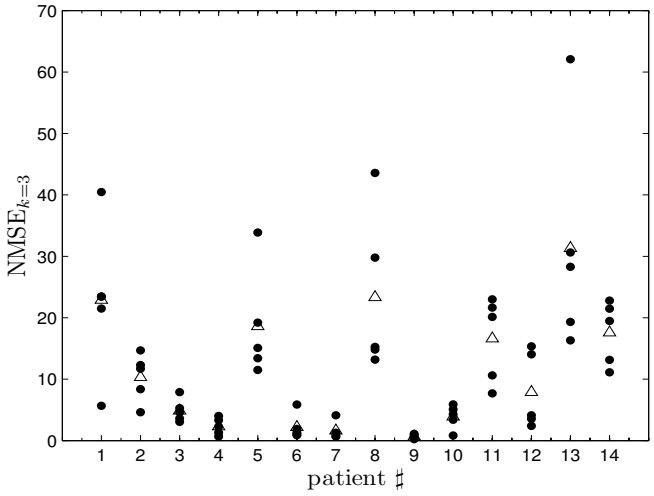

Fig. 7. Values of NMSE$_{k=3}$ in segments 2 up to 6 for all patients in the dataset (•). Mean values are also shown for each patient (△).

$s = 2, \ldots, 6$), while mean $k_{0.95}$ was calculated averaging over segments $s = 1, \ldots, 6$). No significant correlation was found between both $k_{0.95}$ and NMSE$_{k=3}$, respectively, with the energy of the segments. Again, no significant correlation was found between the difference of NMSE$_{k_{0.95}}$ − NMSE$_{k=3}$ and $k_{0.95}$.

Fig. 6 shows the values of $k_{0.95}$ in segments 1 to 6 for each analysed patient, while Fig. 7 shows the values of NMSE$_{k=3}$ in segments 2 to 6 for each analysed patient. Disparities in the number of displayed points per patient are due to equal and then superposed values (relative to $k_{0.95}$), or very close values (relative to NMSE$_{k=3}$).

B. Noninvasive Classification of AF

Cluster analysis was carried out on the mean values of parameters $k_{0.95}$ ($s = 1, \ldots, 6$) and NMSE$_{k=3}$ ($s = 2, \ldots, 6$) for each patient. Fig. 8 shows the output of the cluster analysis. Two clusters were identified in the ensemble of data. Hence, two groups characterized by different types of AF organization were identified, the first (•) describing more organized AF, characterized by low complexity and high stationarity (or repetitiveness of the PCA mixing matrix), at fixed complexity $k = 3$, across the BSPM recording (low NMSEs), while the second (×) characterized by higher complexity and lower stationarity (higher NMSEs), at fixed complexity. Parameter NMSE$_{k=3}$ appeared more discriminant than $k_0.95$ in distinguishing between the two clusters (points not superposed compared to this parameter). In order to test it, a second cluster analysis was carried

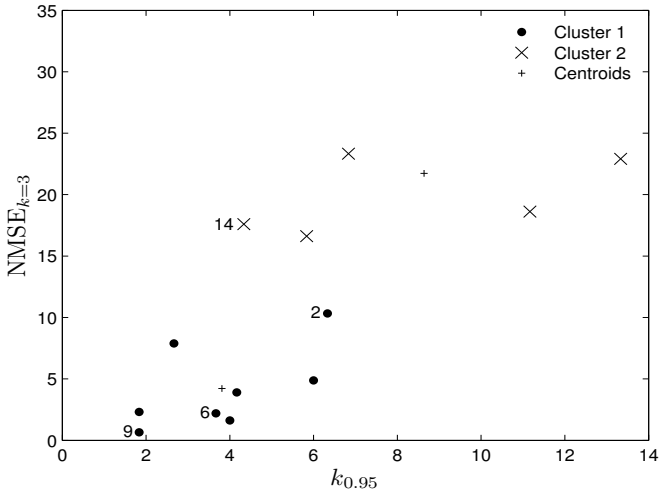

Fig. 8. Cluster analysis based on parameters $k_{0.95}$ and $\mathrm{NMSE}_{k=3}$. Cluster 1 (•) associated to more organized AF (low complexity and high stationarity across the BSPM recording, or low NMSEs), and Cluster 2 (×) associated to less organized AF (higher complexity and lower stationarity, higher NMSEs), are shown. Misclassified patients are highlighted in the figure by their number.

TABLE I
PCA BASED AND WPM BASED CLASSIFICATION OF ALL AF ORGANIZATIONS

Patient ♯	PCA based	WPM based
Patient 1	II/III	II/III
Patient 2	I	II/III
Patient 3	I	I
Patient 4	I	I
Patient 5	II/III	II/III
Patient 6	I	II/III
Patient 7	I	I
Patient 8	II/III	II/III
Patient 9	I	II/III
Patient 10	I	I
Patient 11	II/III	II/III
Patient 12	I	I
Patient 13	II/III	II/III
Patient 14	II/III	I

out exploiting $\mathrm{NMSE}_{k=3}$ only, which produced the same two cluster as the previous one.

In order to compare our results with those obtained by Guillem *et al.* on the same dataset [14], patients belonging to the first cluster were identified as AF type I, while those belonging to the second cluster as AF type II/III, relatively to the Konings' types of wavefront propagation patterns reflected on the surface ECG. Table I summarizes the results of the AF organization classification of each patient given by both studies. Notice that 10 out of 14 patients have been classified in the same way by both methods, 5 as AF type I, and 5 as AF type II/III ($\tilde{7}1\%$ of agreement), while 4 out of 14 have been differently classified. Precisely, patient 14 has now been classified as AF type II/III instead of type I, while patients 2,6, and 9 have now been classified as AF type I instead of II/III. Then, the classification proposed in this study (PCA based) identified 8 patients as AF type I and 6 as AF type II/III, while it was the opposite for the classification given by Guillem (Wavefront Propagation Maps based, or WPM based), as reported in Section II-F.

A Whelch's t-test was performed on the variances of parameters $k_{0.95}$ and $\mathrm{NMSE}_{k=3}$ over all the AA segment recordings for each patient, grouped as the two clusters. By means of this analysis, the differences in the variances of the two parameter values, previously observed in Fig. 8, and introduced in Section III-A, were investigated. A significant difference was observed for parameter $\mathrm{NMSE}_{k=3}$ ($p < 0.01$) between the two clusters, as portrayed in Fig. 9. This underlines the significant difference in terms of reconstruction error, and then stationarity, between different types of AF, and the suitability of this parameter in discriminating between them. Table II summarizes the statistics of the two parameters (mean±SD) for each obtained cluster.

TABLE II
MEAN PARAMETER VALUES FOR THE AA SPATIO-TEMPORAL ANALYSIS, WITH $k = 3$

Parameter	AF I	AF III	p-value
$k_{0.95}$	3.81±1.71	8.64±3.49	$p < 0.01$
$\text{NMSE}_{k=3}$	4.22±3.35	21.73±5.46	$p < 10^{-4}$

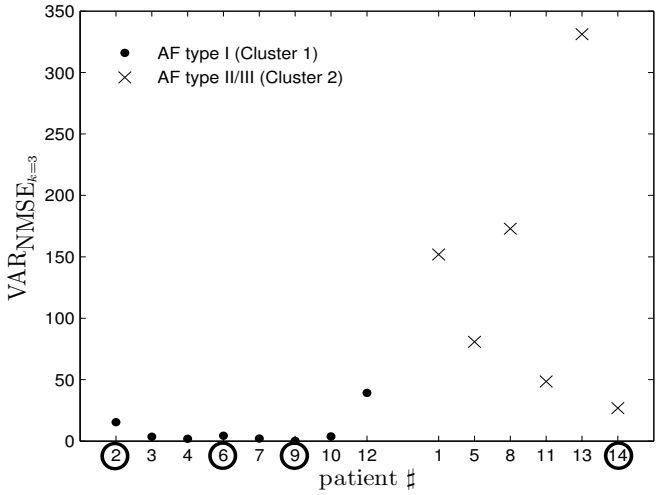

Fig. 9. Variances of parameter $\text{NMSE}_{k=3}$ over all segments in the same patient, grouped according to cluster analysis in order to visually overemphasize their significant difference between the two clusters. Misclassified patients are circled in the figure.

Rounded numbers of $k_{0.95}$ are 4 for the first cluster (squares, range 1 to 11) and 9 for the second cluster (triangles, range 3 to 17).

IV. DISCUSSION

Although the degree of organization in the AA during AF has been observed to be related to its chronification and then potentially to better lead its treatment, there is not nowadays a standard noninvasive procedure to assess AF organization, despite its potential relevance in clinical decision making. This work put forward a novel automated approach to noninvasively evaluate the degree of spatio-temporal organization in the AA during AF. A quantitative evaluation of AA organization was carried out by means of PCA by assessing the spatial complexity and temporal stationarity of the wavefront patterns on the surface ECG. Complexity and stationarity were investigated through novel parameters evaluating the structure of the mixing matrices derived by the PCA of the different AA segments across the BSPM recording. Positive results encourage further research efforts into noninvasive and quantitative AF analysis approaches exploiting spatial diversity. In this sense, the high positive correlation observed for parameters $k_{0.95}$ and $\text{NMSE}_{k=3}$, evaluating the spatial complexity and temporal repetitiveness of the mixing matrix, respectively, makes them suitable to distinguish among different AA organizations. Moreover, their robustness, suggested by the independence of complexity on both the amount of noise in the signal and the procedure, as underlined in Section III-A, makes them worthy of been exploited to distinguish between different types of AF. This is confirmed by the significant difference in the variances of $\text{NMSE}_{k=3}$ observed for the two obtained clusters, underlining the higher stationarity of more organized AF, as shown in Fig. 9.

A. Comparison with Invasive Studies

Results presented in Section III-B on the number of significant components derived for each cluster are consistent with those presented by Faes *et al.* [12]. In that study, using PCA, single-lead electrograms of more organized AF were shown to be represented by a reduced number of principal components. Interestingly, both studies obtained the same results in terms of number of significant components necessary to describe 95% of the variance in the AA (4 for AF type I, and 9 for AF type II/III). Nonetheless, since analysing single-lead electrograms, Faes *et al.* presented a local measure of the temporal organization of AF. On the contrary, this study introduced a noninvasive global measure of the spatio-temporal organization of the whole AA inside the atria.

B. Comparison with Noninvasive Studies

The possibility of analysing the global activity of the atria through noninvasive recordings during AF has been widely observed [24]. The noninvasive assessment of human AF organization through Holter ECG recordings was previously described by Alcaraz *et al.*, both in the attempt of predicting the spontaneous termination of paroxysmal AF [25], and of describing the paroxysmal atrial fibrillation time variation [26]. However, since the use of a limited number of leads could prevent from exploiting the spatial diversity of multi-lead ECGs and might not be always representative of the voltages that can be recorded from the whole body surface, additional information extracted from several sites is required, as inferred in [14]. In line with this study, our observations have confirmed the possibility of identifying several activation patterns with different organization degrees by exploiting the spatial diversity within BSPM recordings, despite the low signal-to-noise ratio of AF signals.

AF type classification of the same dataset performed by Guillem *et al.* and authors, respectively, showed high similarity (10 out of 14 patient equally classified), strengthening the results of both methods, and pointing out the importance of the high spatial diversity offered by BSPM recordings. Misclassified patients might be due to the different temporal resolutions employed by the two methods. Indeed, in [14] each cycle was analyzed individually (160-ms for a typical atrial dominant cycle length, but it varies for each patient), compared with 10-s employed in this study. Supposing that also AF type I might sometimes present more complex activity, even if keeping its organized state on the whole, a high temporal resolution analysis could by accident analyse short segments presenting this infrequent complexity, interpreting it as a more disorganized AF. This could be prevented by carrying the analysis on longer segments, more able to extract the average state of complexity of the underlying atrial activations.

However, this method is not suitable to estimate the pattern directions of the propagating atrial wavefronts, invasively identified by Konings *et al.*, and visually observed by Guillem *et al.* on surface BSPM recordings. Nonetheless, it appears useful for quantifying the degree of AA organization during AF, providing information on the chronification of the arrhythmia, and then to be useful for improving AF diagnosis and treatment, reducing risks related to invasive recordings, as well as health care costs.

C. General Remarks and Limitations

Different studies based on invasive recordings have shown that the atrial electrical activity during AF presents a significant spatial inhomogeneity, with coexistence of atrial areas characterized by different AA organization, which is more evident in patients with paroxysmal AF [3], [5], [6], [12]. Particularly, in patients with chronic AF, a shortening of the AA intervals and a greater prevalence of disorganized activity in all the atrial sites examined was observed. However, in patients with paroxysmal AF, a significant dispersion of refractoriness was observed [6]. Direct correlation of our observations with these findings cannot be inferred for the lack of simultaneous invasive recordings, so that the actual mechanisms of AF in each patient are unknown. Moreover, the dataset is composed by only persistent AF recordings. Nonetheless, we might expect that the global perspective on the underlying AA given by surface ECG recordings mainly reflects the behaviour of the atrial areas characterized by an AF type similar to the predominant one observed on the body surface.

One limitation of this study is the absence of simultaneous electrograms in order to have an objective reference for a Koning's-like classification of the patients in different AF classes. A second limitation is that the method was applied only on the TQ segments in the BSPM recording. This was done in order to avoid interferences on the estimation of the complexity due to the presence of QRS complex residues in the remainder ECG, since a QRS-T cancellation or AA extracting method able to produce a remainder ECG free from QRS residues still does not exist. Moreover, AA extracting methods containing a first estimation based on PCA did not look consistent to authors with the analysis presented here, also based on PCA, since the results of the latter could be in some ways biased by the former. Another limitation is that this study was conducted in a consecutive but small series of patients. Nonetheless, significance of the obtained results makes them promising despite the small dataset. Finally, despite of the undeniable usefulness of the high spatial resolution given by BSPM recordings, the possibility to employ this analysis on standard 12-leads ECGs needs to be assessed in future works. The present method suggests that automated analysis and classification of AF in surface recordings is indeed possible and positive results strongly support the appropriateness of signal processing approaches exploiting spatial diversity in AF analysis.

ACKNOWLEDGMENT

The work of Pietro Bonizzi is supported by the EU by a Marie-Curie Fellowship (EST-SIGNAL program: http://est-signal.i3s.unice.fr) under contract No MEST-CT-2005-021175. The work of Maria S. Guillem, Andreu M. Climent and Francisco Castells is supported by a Spanish Ministry of Science and Innovation under EASI (TEC2008-02193/TEC).

REFERENCES

[1] G. Moe, "On the multiple wavelet hypothesis of atrial fibrillation," *Arch. Int. Pharmacodyn. Ther.*, vol. 140, pp. 83–188, 1962.

[2] M. A. Allessie, W. E. J. E. P. Lammers, F. I. M. Bonke, and J. Hollen, *Cardiac Electrophysiology and Arrhythmias*. Grune & Stratton, Orlando, Florida, 1985, ch. Experimental evaluation of Moe's multiple wavelet hypothesis of atrial fibrillation, pp. 265–275.

[3] F. Censi, V. Barbaro, P. Bartolini, G. Calcagnini, A. Michelucci, G. Gensini, and S. Cerutti, "Recurrent patterns of atrial depolarization during atrial fibrillation assessed by recurrence plot quantification," *Ann. Biomed. Eng.*, vol. 28, pp. 61–70, 2000.

[4] G. W. Botteron and J. Smith, "A technique for measurement of the extent of atrial activation during atrial fibrillation in the intact human heart," *IEEE Trans. Biomed. Eng.*, vol. 42, pp. 579–586, 1995.

[5] H. Li, J. Hare, K. Mughal, D. Krum, M. Biehl, S. Deshpande, A. Dhala, Z. Blanck, J. Sra, M. Jazayeri, and M. Akhtar, "Distribution of atrial electrogram types during atrial fibrillation: Effect of rapid atrial pacing and intercaval junction ablation," *J. Amer. Coll. Cardiol.*, vol. 27, pp. 1713–1721, 1996.

[6] F. Gaita, L. Calò, R. Riccardi, L. Garberoglio, M. Scaglione, G. Licciardello, L. Coda, P. Di Donna, P. Bocchiardo, D. Caponi, L. Antolini, F. Orzan, and G. Trevi, "Different Patterns of Atrial Activation in Idiopathic Atrial Fibrillation: Simultaneous Multisite Atrial Mapping in Patients With Paroxysmal and Chronic Atrial Fibrillation," *J Am Coll Cardiol*, vol. 37, pp. 534–541, 2001.

[7] A. Bollmann, "Quantification of electrical remodeling in human atrial fibrillation," , vol. 47, pp. 207–209, 2000.

[8] V. Fuster, L. E. Ryden, D. Cannom, H. Crijns, and A. e. a. Curtis, "ACC/AHA/ESC 2006 guidelines for the management of patients with atrial fibrillation: A report of the American College of Cardiology/American Heart Association Task Force on practice guidelines and the European Society of Cardiology Committee for practice guidelines (writing committee to revise the 2001 guidelines for the management of patients with atrial fibrillation): developed in collaboration with the european heart rhythm association and the heart rhythm society," *Circulation*, vol. 114, pp. e257–e354, 2006.

[9] T. Everett, J. Moorman, L. Kok, J. Akar, and D. Haines, "Assessment of global atrial fibrillation organization to optimize timing of atrial defibrillation," *Circulation*, vol. 103, pp. 2857–2861, 2001.

[10] J. L. Wells, R. Karp, N. Kouchoukos, W. Maclean, T. James, and A. Waldo, "Characterization of atrial fibrillation in man: studies following open-heart surgery," *PACE*, vol. 1, pp. 426–438, 1978.

[11] K. Konings, C. Kirchhof, J. Smeets, H. Wellens, O. Penn, and M. Allessie, "High-density mapping of electrically induced atrial fibrillation in humans," *Circulation*, vol. 89, pp. 1665–1680, 1994.

[12] L. Faes, G. Nollo, M. Kirchner, E. Olivetti, F. Gaita, R. Riccardi, and R. Antolini, "Principal component analysis and cluster analysis for measuring the local organisation of human atrial fibrillation," *Med. Biol. Eng. Comput.*, vol. 39, pp. 656–663, 2001.

[13] A. Bollmann, D. Husser, L. Mainardi, F. Lombardi, P. Langley, A. Murray, J. J. Rieta, J. Millet, S. Bertil Olsson, M. Stridh, and L. Sornmo, "Analysis of surface electrocardiograms in atrial fibrillation: techniques, research, and clinical applications," *Europace*, vol. 8, pp. 911–926, 2006.

[14] M. Guillem, A. Climent, F. Castells, D. Husser, J. Millet, A. Arya, C. Piorkowski, and A. Bollmann, "Noninvasive mapping of human atrial fibrillation," *J Cardiovasc Electrophysiol*, vol. , pp. 1–7, 2009.

[15] R. Lux, "Electrocardiographic body surface potential mapping," *Crit Rev Biomed Eng*, vol. 8, pp. 253–279, 1982.

[16] S. Maynard, I. Menown, G. Manoharan, J. Allen, A. McC, and A. Adgey, "Body surface mapping improves early diagnosis of acute myocardial infarction in patients with chest pain and left bundle branch block," *Heart*, vol. 89, pp. 998–1002, 2003.

[17] B. Khaddoumi, H. Rix, O. Meste, M. Fereniec, and R. Maniewsky, "Body Surface ECG Signal Shape Dispersion," *IEEE Trans Biomed Eng*, vol. 53, pp. 2491–2500, 2006.

[18] F. Castells, P. Laguna, L. Sörnmo, A. Bollmann, and J. M. Roig, "Principal component analysis in ecg signal processing," *EURASIP J. Appl. Signal Process.*, vol. 2007, no. 1, pp. 98–98, 2007.

[19] P. Bonizzi, R. Phlypo, V. Zarzoso, O. Meste, and A. Fred, "Atrial Signal Extraction In Atrial Fibrillation ECGs Exploting Spatial Constraints," in *Proc. Eusipco*, vol. 16, 2008.

[20] P. Bonizzi, R. Phlypo, V. Zarzoso, and O. Meste, "The exploitation of spatial topographies for atrial signal extraction in atrial fibrillation ECGs," in *Proc. IEEE EMBS*, vol. 30, 2008, pp. 1867–1870.

[21] L. Sörnmo and P. Laguna, *Bioelectrical Signal Processing in Cardiac and Neurological Applications*. Amsterdam: Elsevier Academic Press, 2005.

[22] J. Rieta, C. Sánchez, J. Sanchis, F. Castells, and J. Millet, "Mixing matrix pseudostationarity and ECG preprocessing impact on ICA-based atrial fibrillation analysis," *Lecture Notes in Computer Science*, vol. 3195, p. 10791086, 2004.

[23] P. Okin, M. Malik, K. Hnatkova, E. Lee, J. Galloway, B. L.G., H. B.V., and D. R.B., "Repolarization abnormality for prediction of all-cause and cardiovascular mortality in American Indians: the Strong Heart Study," *J Cardiovasc Electrophysiol*, vol. 16, pp. 945–51, 2005.

[24] S. Petrutiu, J. Ng, G. Nijm, H. Al-Angari, S. Swiryn, and A. Sahakian, "Atrial Fibrillation and Waveform Characterization. A Time Domain Perspective in the Surface ECG," *IEEE Eng Med Biol Mag*, vol. 25, pp. 24–30, 2006.

[25] R. Alcaraz and J. Rieta, "Wavelet bidomain sample entropy analysis to predict spontaneous termination of atrial fibrillation," *Physiol Meas*, vol. 29, pp. 65–80, 2008.

[26] ——, "Non-invasive organization variation assessment in the onset and termination of paroxysmal atrial fibrillation," *Comput Methods Programs Biomed*, vol. 93, pp. 148–154, 2009.